Colloids and Surfaces B: Biointerfaces 172 (2018) 699–707

Contents lists available at ScienceDirect

Colloids and Surfaces B: Biointerfaces

journal homepage: www.elsevier.com/locate/colsurfb

Design and characterization of immobilized biocatalyst with lipase activity onto magnetic magnesium spinel nanoparticles: A novel platform for biocatalysis

C.M. Romero[a,b,*], F.C. Spuches[a,1], A.H. Morales[a,1], N.I. Perotti[a], M.C. Navarro[b], M.I. Gómez[b]

[a] PROIMI-CONICET, Av. Belgrano y Pasaje Caseros, T4001 MVB, Tucumán
[b] Facultad de Bioquímica, Química y Farmacia, UNT. Chacabuco 461, T4000ILI, San Miguel de Tucumán, Argentina

ARTICLE INFO

Keywords:
Lipase
Immobilization
Magnetic magnesium spinel nanoparticle
Novel biocatalyst

ABSTRACT

Lipases (EC 3.1.1.3) are very used industrial enzymes but presents drawbacks such as lack of stability, and poor recyclability. Most of these obstacles can be solved by lipase immobilization. The objective of this work was evaluated to magnetic magnesium spinel nanoparticles as support for lipase immobilization by covalent bound. The techniques used for nanoparticles synthesis presented advantages in the size selection of the nanoparticles obtained (60–100 nm). The immobilization of *Candida rugosa* lipase (CRL) was optimized. The optimal conditions were determined to be pH 3.7, enzyme concentration of 1.1 mg/mL at 4 °C and an ionic strength of 100 mM. The CRL@$MgFe_2O_4$ activity obtained was 3.2 times over the starting conditions (4.03 U/mL). The immobilization of the lipase on Fe_3O_4 was evaluated and compared. The activity of the CRL@$MgFe_2O_4$ was 61% higher than CRL@Fe_3O_4 and 22% higher than free enzyme. CRL@$MgFe_2O_4$ improved the lipase stability at alkaline pH, hydrophilic solvent and high temperatures. The thermogravimetric analysis showed that this new biocatalyst was more stable compared to the free enzyme. Additionally, the immobilized lipase was recycled by magnetic force and used in ten catalysis cycles. The performance of the recycle was improved using butanol or Triton X 100 during washing. Finally, CRL@$FeMg_2O_4$ showed hydrolysis and synthesis activity. Thus, CRL@$FeMg_2O_4$ as a novel biocatalyst generation presents interesting properties for industrial applications.

1. Introduction

Lipases (Triacylglycerol Acyl Hydrolase EC 3.1.1.3) are one of the most used industrial enzymes. They have many applications in the manufacture of a wide range of products [1]. Lipases are produced in high yields by animals, plants and microbial organisms. Because of their excellent properties such as chemoselectivity, regioselectivity and stereoselectivity, lipases are widely used as biocatalysts in hydrolysis and synthesis reactions [2].

However, the use of free lipases presents numerous drawbacks such as lack of stability, difficult separation, and poor recyclability, which interferes with a wider commercial use of these enzymes. Most of these obstacles could be avoid by immobilization of lipases onto solid materials [3,4].

In the last year, there was a considerable progress in the field of interactions between enzymes and nanomaterials or nanoparticles [5]. Nanoparticles have been widely studied for adjusting the enzymatic structure and conserved the activity of the enzyme. Enzymatic immobilization on nanoparticles based on suitable design and optimization can significantly enhance enzymatic catalytic performance.

Nanoparticles of metal oxide are serving as novel matrices for enzyme immobilization [6]. These types of nanoparticles are excellent supports for enzyme stabilization due to their small size and large surface area [7,8]. Among the metal oxides nanoparticles, the magnetic oxides have been used as support in the biotechnological and biomedical fields to facilitate the substrate and product recovery [9,7].

Magnetic nanoparticles possess unique properties of nontoxicity and biocompatibility. This is the reason that they are used as support for lipase immobilization, providing a large surface area for potential high enzyme loading and selective separation from the reaction mixture under magnetic field. Magnetite (Fe_3O_4) is one of the magnetic nanoparticles most used for enzyme immobilization [4].

* Corresponding author at: PROIMI-CONICET, Av. Belgrano y Pasaje Caseros, T4001 MVB, Tucumán Fac. Bioq., Qca. y Farmacia (UNT), Ayacucho 461, 4000, Tucumán, Argentina.
E-mail address: cinromero78@gmail.com (C.M. Romero).
[1] Contributed equally to this work.

https://doi.org/10.1016/j.colsurfb.2018.08.071
Received 2 January 2018; Received in revised form 24 June 2018; Accepted 18 August 2018
Available online 15 September 2018
0927-7765/

However, there is a continuous search of new magnetic nanoparticles. In this sense, different ferrites magnetic nanoparticles have been evaluated as a novel support for enzyme immobilization [10]. Magnesium ferrite ($MgFe_2O_4$) is a cubic spinel ferrite nanoparticle, wherein the tetrahedral and octahedral cation sites are coordinated and occupied by divalent Mg^{2+} and trivalent Fe^{3+}, respectively [11]. The nanoparticles of $MgFe_2O_4$ present high stability, cost-efficiency, and non-toxicity. Moreover, they are insoluble in water and show high adsorption capacity in addition to a typical superparamagnetic behavior at room temperature [12].

In spite of, all the advantages of magnetic nanoparticles when they are used as support for enzymes immobilization, is highly necessary adjusting several parameters to preserves the enzymatic activity such as the size control and dispersion of magnetic nanoparticles because they often suffer aggregation with diminish of magnetic properties [4].

In this work, magnesium ferrite nanoparticles were synthesized and evaluated as support for a lipase immobilization. This study is the first part of a novel technology platform where the ferrite magnetic nanoparticles are tested for the design of new generation biocatalysts.

2. Materials and methods

2.1. Materials

Lipase (EC 3.1.1.3), from *Candida rugose* lipase (CRL), bovine serum albumin (BSA), (3-Aminopropyl) triethoxysilane (APTES), Coomassie Blue G-250 Triolein, p-nitrophenylpalmitate (p-NPP), Triton X 100 were purchased from Sigma-Aldrich. All analytical grade solvents were used without further purification.

2.2. Synthesis of magnetic magnesium spinel: $MgFe_2O_4$

The synthesis of the mixed oxide used as magnetic support was made from the thermal decomposition of the inorganic complex pentacyanocyanilferrate of magnesium, ($Mg[Fe(CN)_5NO]\cdot 4H_2O$). It was prepared in two stages:

2.2.1. Synthesis of complex $Mg[Fe(CN)_5NO]\cdot 4H_2O$

$Mg[Fe(CN)_5NO]\cdot 4H_2O$ was prepared by the indirect method from silver pentacyanocyanilferrate, as it cannot be obtained directly from sodium pentacyanocyanilferrate.

The double substitution reactions are:

$$[Fe(CN)_5NO]^{2-}_{(aq)} + 2\ Ag^{+}_{(aq)} \rightarrow Ag_2[Fe(CN)_5NO]_{(s)}$$

$$Ag_2[Fe(CN)_5NO]_{(s)} + Mg^{2+}_{(ac)} + 2\ Cl^{-}_{(ac)} \rightarrow Mg^{2+}_{(ac)} + [Fe(CN)_5NO]^{2-}_{(ac)} + 2\ AgCl_{(s)}$$

The obtained solution was separated from the solid by centrifugation and concentrated by evaporation. Magnesium pentacyanocyanilferrate was synthesized as a reddish crystalline compound very soluble in water; it was stabilized in a drier under silica gel.

2.2.2. Synthesis of mixed oxide $MgFe_2O_4$ nanoparticles

$MgFe_2O_4$ mixed oxide was obtained by the thermal decomposition of $Mg[Fe(CN)_5NO]\cdot 4H_2O$ in air. The sample was introduced into the furnace at 600 °C (end temperature), then remained there for 10 h and cooled to room temperature.

2.3. Surface modification of magnetic magnesium spinel

$MgFe_2O_4$ nanoparticles were prepared in aqueous solution with agitation and then treated with APTES knowing that the optimal surface modification molar ratio of APTES to $MgFe_2O_4$ was 4:1. The resulting suspension was stirred (150 rpm) at 70 °C for 2 h. After that the suspension was cooled at room temperature, the prepared APTES-modified $MgFe_2O_4$ were collected with a magnet and washed three times with deionized water.

For preparation of aldehyde-functionalized $MgFe_2O_4$, glutaraldehyde was used as the reagent for surface modification of functionalized $MgFe_2O_4$. To do this, 100 mg of APTES-modified $MgFe_2O_4$ were suspended in 10 mM buffer phosphate pH 7, and then 0.4 mL of glutaraldehyde 25% was added and mixed for 4 h ta room temperature. After thoroughly washed with 1 mol/L saline solution, $MgFe_2O_4$ were dried at 45 °C during 24 h. The resulting materials were collected as functionalized supports for lipase immobilization.

2.4. Immobilization of lipase

2.4.1. Screening of variables by placket-burman design (PBD)

Screening designs are commonly used when little is known about a system or process. A 6-factor 24-run (12 mixtures with respective random duplicated) Plackett-Burman statistical design at two levels was generated using MINITAB 17 statistical experiment design software.

The independent variables evaluated in this study and their respective levels are listed in Supplemental Material (TS1). Each of these variables was represented with a code (X) and two levels which were denoted by (+1) and (−1). The response evaluated in the present work was hydrolysis activity (Y). A statistical analysis was performed with data from immobilized biocatalysts hydrolysis reaction obtained at each condition of the design. Both the *t*-test and *p* value at a 95% significance level were used to confirm the significance of the factors studied. The coefficient of determination, R^2, was used to see how well data fit the model.

2.4.2. Optimization of immobilization: response surface methodology (RSM)

A Response Surface Methodology (RSM), using a Box-Behnken design, was adopted to evaluate the interactions and identify the optimal enzyme concentration (A), ionic strength (B), and pH (C) that affect the immobilization of the biocatalyst. These variables at three different levels (+1, 0, −1) and the schedule for the model are shown in TS2 (Supplemental Material).

2.5. Enzyme assays

2.5.1. Lipase activity

Lipase activity was measured using p-NPP as substrate. Free lipase (100 μL) or immobilized lipase (0.005 g.) was added to 1 mL of buffer A: 100 mM buffer phosphate (pH 7) containing 1 mM p-NPP, 0.1% (w/v) gum arabic and 0.4% (w/v) Triton X-100 [13]. The reaction mixture was shaken (150 rpm) at 37 °C for 10 min. For immobilized enzyme, the mixture was centrifuged for 30 s (10.000 rpm) to terminate the reaction. The p-nitrophenyl (p-NP) released as a result of enzymatic hydrolysis was estimated spectrophotometrically at 405 nm. One unit of enzyme activity (U) was defined as the amount of biocatalyst that released 1 μmol of p-nitrophenol per minute under the standard assay conditions.

2.5.2. Protein determination

Protein estimation was evaluated by Bradford method [14]. 500 μL of Coomassie Blue G-250 reagent was added to 500 μL of sample. After, the mixture was incubated for 10 min at room temperature. Finally the protein concentration was estimated at 595 nm using bovine serum albumin (fraction V) as standard.

2.6. Characterization of magnetic magnesium spinel nanoparticles and immobilized lipase ($CRL@MgFe_2O_4$)

2.6.1. FTIR spectra analysis

Fourier transform infrared (FTIR) analysis of $Mg[Fe(CN)_5NO]$ precursor, $MgFe_2O_4$, $MgFe_2O_4$ functionalized and $CRL@MgFe_2O_4$ were monitored by using Perkin Elmer 1600 FTIR spectrometer in the

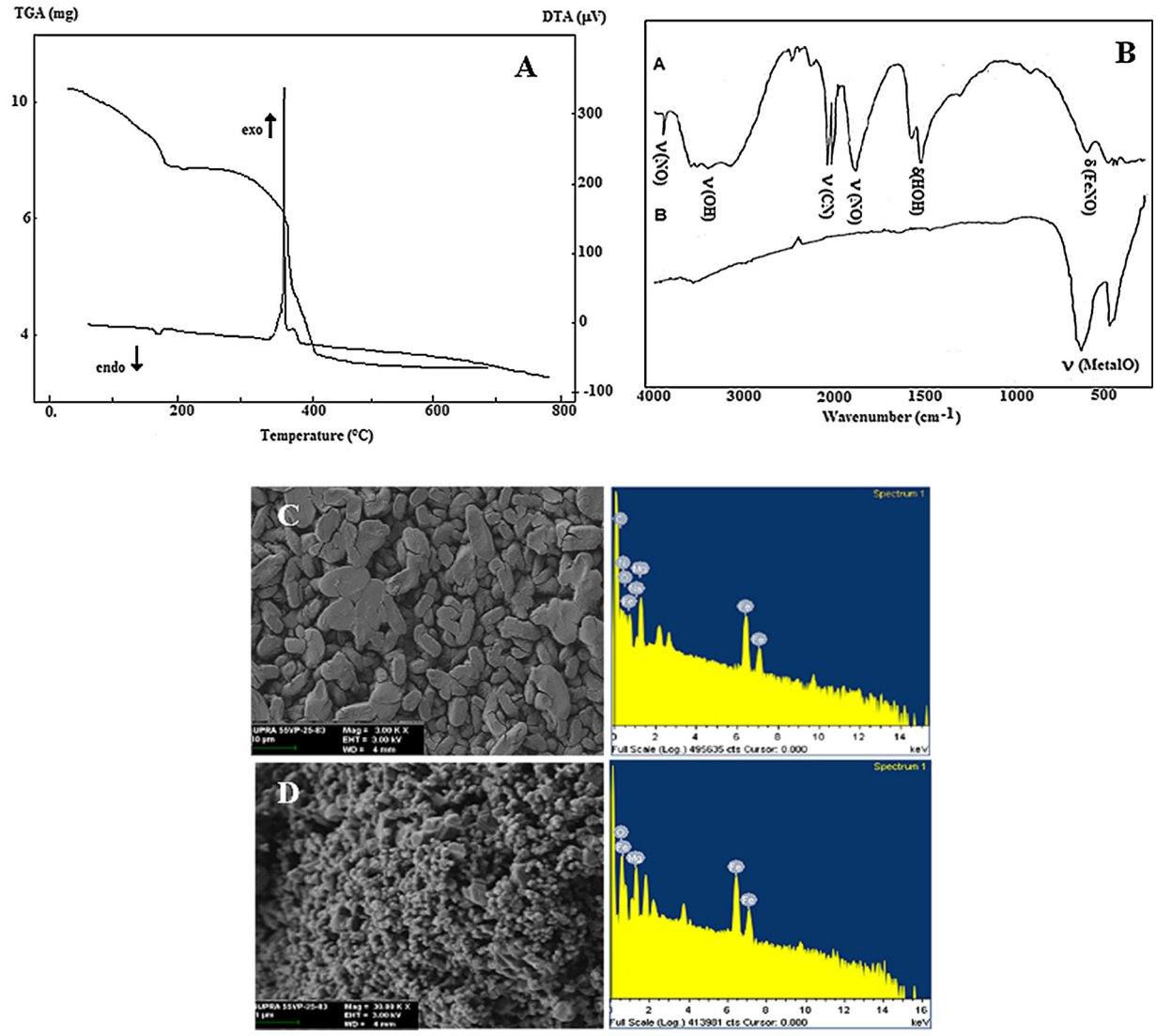

Fig. 1. A- TGA and DTA of decomposition process of $Mg[Fe(CN)_5NO]{\cdot}4H_2O$ complex. B- FTIR spectra of $Mg[Fe(CN)_5NO]{\cdot}4H_2O$ precursor (a) and synthetized nanoparticles of $MgFe_2O_4$ (b). C-SEM (3.00 K ×) and EDS of $Mg[Fe(CN)_5NO]{\cdot}4H_2O$ precursor. D- SEM (33.00 K ×) and EDS of $MgFe_2O_4$ nanoparticles.

frequency range of 4000–400 cm^{-1} at the Physic-Chemistry Institute from Faculty of Biochemistry, Chemistry and Pharmacy (National Tucumán University). The standard KBr pellet technique was applied for sample preparation.

2.6.2. Scanning electron microscopy (SEM) and energy-dispersive X-ray spectrometry (EDS)

The size, shape, morphology and distribution of the nanoparticles and immobilized enzyme were analyzed by SEM using JEOL JSM-35 CF, and EDS and elemental mapping with an Inca Penta FET X 3, Oxford instrument, from Laboratory of Electronic Microscopy (CIME) from CONICET-UNT.

2.6.3. Thermogravimetric analysis (TGA)

The thermal decomposition processing was examined by thermogravimetric analysis (TGA) and differential thermal analysis (DTA) in Shimadzu TGA/DTA-50 equipments in the temperature range from 25 to 800 °C at a heating rate of 5°/min under air flowing

2.6.4. Stability assays

The effect of pH on the activity of free and immobilized lipase was tested at 37 °C for 1 h in the pH range of 3–10, using the following 100 mM buffers: KCl − HCl (pH 2), citrate-citric acid (pH 3 and 4), phosphate (pH 6–8) and borate − HCl (pH 9 and 10). On the other hand, measurements of enzyme activity were carried out in standard reaction mixture at different temperatures. The immobilized enzyme was pre-incubated in 100 mM phosphate buffer (pH = 7.0) for 1 h at different temperatures covering the range of 10–70 °C. Finally, 50% (v/v) of organic solvents, methanol, ethanol, isopropanol, butanol, glycerol, acetone and n-hexane, were incubated with free and immobilized lipase at the same time at 37 °C. Residual activity was then calculated considering the enzyme activity at time zero as 100%.

2.6.5. Biocatalyst reuse

The reusability of CRL@$MgFe_2O_4$ was studied under the same conditions as described in the activity assay section. After each run, CRL@$MgFe_2O_4$ was magnetically separated and washed with different solvents: Buffer A, butanol, acetone and ethanol (100%) to remove any remaining products or substrate species. The residual enzyme activity after each cycle was normalized to the initial value of 100%.

2.7. Application of the CRL@$MgFe_2O_4$ in hydrolysis and transesterification reaction

For lipid hydrolysis, an emulsion was prepared by dispersing triolein 50 mM in an aqueous solution of polyvinyl alcohol (PVA; 20 g/L)

by sonication. For triolein hydrolysis, the reaction was started by the addition of 200 µL of the emulsion and 800 µL of the free CRL in phosphate buffer 50 mM pH 7.0 (0.2 mg of lyophilized enzyme per mL of buffer; 100 U/mL). For the immobilized CRL, 25 mg of the biocatalyst (15 U/mg) was added to 200 µL of emulsion and 800 µL of phosphate buffer 50 mM pH 7.0. Reaction was carried out at 37 °C for 30, 60, 120 and 180 min and stopped by the addition of 1000 µL of an ethanol:sulphuric acid solution (100:0.8, v/v). Lipid-soluble compounds were extracted with 2 mL of hexane and stored at −20 °C.

The ethanolysis reaction was carried out in closed Erlenmeyer flasks (250 mL) containing the substrate consisting of soybean oil and anhydrous ethanol at 1:6 M ratio using n-hexane as a solvent. The assays conditions were 45 °C, 72 h under reciprocal shaker (170 rpm). The immobilized biocatalyst represented 20% of the total mass of the reaction mixture. The addition of alcohol was carried out in three feeds, in 24 h intervals. Qualitative analysis of products of hydrolysis or synthesis reaction were analyzed by thin layer chromatography (TLC) on silica gel 60 using n-hexane: ethyl acetate: acetic acid (90:10:1) as developing solvent. Spots were visualized in iodine vapor.

3. Result and discussion

3.1. Characterization of magnesium spinel

The magnesium ferrite ($MgFe_2O_4$) was obtained by the thermal decomposition method of the $Mg[Fe(CN)_5NO]$ complex.

This method of preparation is very advantageous compared to other synthesis methods reported to obtain mixed oxides [15–17], since it produces powders with homogeneous particle size, in the order of nanometers at a relatively low temperature (600 °C). In addition, by placing the sample in the oven when it has reached the final temperature, the decomposition process is very fast and violent; this reduces the formation of intermediary species such as carbonates [18].

TGA and DTA data for $Mg[Fe(CN)_5NO]\cdot 4H_2O$ are shown in Fig. 1A. The decomposition process follows two steps. The first one ends at 200 °C with a weight loss of 22.81% corresponds to the dehydration process to obtain the anhydrate (theoretical value 23.10%). This corresponds to the endothermic process observed at the same temperature range in the DTA. The second stage starts at 280 °C and ends at 600 °C, corresponds to 39.80%, involves the elimination of cyanide and nitrosyl groups, (theoretical value 40.28%), in the DTA a very sharp and exothermic peak is observed, which indicates that the reaction is abrupt. The total loss is 62.61% corresponding to the formation of $MgFe_2O_4$ from the precursor complex (theoretical value 61.94%). Subsequently no weight losses are recorded, that is, a stable product was obtained.

The FTIR spectra corresponding to the precursor complex and the mixed oxide obtained from its thermal decomposition are shown in Fig. 1B.

The peaks whose assignments belong to the presence of various functional groups such as CN, H_2O and NO for $Mg[Fe(CN)_5NO]\cdot 4H_2O$ and Metal-O for $MgFe_2O_4$ are shown in TS3 (Supplemental Material). In addition, the total lack of the peaks corresponding to the precursor is observed in Fig. 1B, confirming the formation of the oxide.

The morphologies of $Mg[Fe(CN)_5NO]\cdot 4H_2O$ precursor (Fig. 1C) and $MgFe_2O_4$ nanoparticles (Fig. 1D) were investigated by SEM. The SEM micrograph of $Mg[Fe(CN)_5NO]\cdot 4H_2O$ powder in Fig. 1C shows that it was made of large polyhedron crystals, well defined with sharp edges up to 10 µm in size. The SEM micrograph of $MgFe_2O_4$ nanoparticles in Fig. 1D shows that the shape of this is quite different with that of its precursor complex. As can be seen, the large polyhedron grains of the complex $Mg[Fe(CN)_5NO]\cdot 4H_2O$ was completely disrupted and extremely small particles appeared, in the order of nanometers, agglomerated together. The % weight obtained by EDS analysis, and theoretical performance of the process is shown in Table 1 and Fig. 1C and D.

Table 1
Results of EDS analysis, % weight obtained and theoretical performance of the $Mg[Fe(CN)_5NO]$, $MgFe_2O_4$ and Immobilized biocatalyst.

Particles	Element	Weight %	Theoretical %
$Mg[Fe(CN)_5NO]$	O	11.48	6.66
	Mg	8.04	10.11
	Fe	20.94	23.24
	C	25.25	24.97
	N	29.47	34.86
$MgFe_2O_4$	O	32.56	32.00
	Mg	16.32	12.15
	Fe	51.12	55.84
Immobilized biocatalyst	O	54.33	51.24
	Mg	13.54	8.40
	Fe	54.32	25.58
	C	32.13	40.36
	N	19.57	20.95

3.2. Lipase immobilization on magnetic nanoparticles of a magnesium spinel: CRL@$MgFe_2O_4$

In this work, (3-aminopropyl) triethoxysilane (APTES) was used as a supporting layer for immobilization. The silanization process occurs between hydroxylated $MgFe_2O_4$ and silane molecule from APTES. Silanization with amine group (NH_2) terminated organosilanes is widely employed due to the high NH_2 group reactivity with different complementary functional groups of the enzyme [19,20].

After the functionalization, the lipase was bound by covalent union to the amino group-nanoparticle by glutaraldehyde. According to PBD results, the variables that showed to significantly affect the lipase immobilization were ionic strength, enzyme concentration, pH and temperature. The ionic strength and the enzyme concentration had a significant effect at highest levels assayed while the pH and temperature had a significant effect at the lower level assayed (Table 2). It was observed that the lipase activity of the immobilized biocatalyst was improved with an enzyme concentration of 0.50 mg/mL, ionic strength of 50 mM, a temperature of 4 °C and pH 4. In this condition, 5.69 ± 0.02 U/mL of Lipase activity were detected (Supplement Material TS1). The variables time and magnetic nanoparticles amount did not show a significant effect and were not considered for posterior optimization assays (Table 2).

For later studies, the temperature was fixed at 4 °C. The ionic strength, enzyme concentration and pH, were selected as independent variables for to evaluate the influence in protein immobilization by RSM design. The lipase activity of the immobilized biocatalyst was the response variable (Supplement Material TS2).

Experimental data were fitted by Design Expert software into a second order polynomial equation to explain the Lipase activity by only considering the significant terms.

$$\text{Lipase Activity} = -53.7 + 0.0163\ \text{IS} + 22.43\ \text{EC} + 29.20\ \text{pH} - 0.000153\ \text{IS*IS} - 9.91\ \text{EC*EC} - 4.188\ \text{pH*pH} - 0.0239\ \text{IS*EC} +$$

Table 2
Effect of variable and statistical analysis of immobilized biocatalyst, CRL@$MgFe_2O_4$ using Plackett–Burman design for hydrolysis reaction.

Code	Variable	Level		Effect (E)	Statistical significance	
		−1	+1		Test t	p Value
A	pH	4	7	−1.475	−2.63	0.017
B	Temperature	4	25	−1.422	−2.54	0.021
C	Reaction time	6	24	1.152	2.06	0.056
D	Enzyme concentration	0.25	0.50	1.622	2.89	0.010
E	MNPs[a]	50	100	0.635	1.13	0.273
F	Ionic Strenght	10	50	2.508	4.48	0.000

[a] MNPs: magnetic nanoparticles.

Table 3
Effect of variable and statistical analysis of immobilized biocatalyst, CRL@$MgFe_2O_4$ using RSM design for hydrolysis reaction.

Code	Variable	Level			Effect (E)	Statistical significance	
		−1	0	1		Test t	p Value
A	IE[a]	50	100	150	0.711	0.91	0.374
B	EC[b]	0.50	1	1.50	1.681	2.15	0.044
C	pH	3	4	5	−5.610	−7.18	0.000
D	IE*IE				−0.766	−0.67	0.513
E	EC*EC				−4.954	−4.31	0.000
F	pH*pH				−8.375	−7.28	0.000
G	IE*EC				−1.195	−1.08	0.293
H	IE*pH				1.133	1.03	0.318
I	EC*pH				0.363	0.33	0.746

[a] **IS**: Ionic Strenght (mM).
[b] **EC**: Enzyme concentration (mg/mL).

$$0.0113\ IS*pH + 0.36\ EC*pH \quad (1)$$

The significance of the quadratic polynomial model was evaluated as is shown in Table 3 observing that pH and enzyme concentration have a significant effect on lipase activity during the immobilization observing that the activity was favored at the lowest pH and at higher enzyme concentration while the ionic strength not showed a significant effect on lipase activity (Fig. 2A).

The lipase showed to be more effective for cross-linking by glutaraldehyde at pH 4. The pH has a profound effect on the polymerization rate of glutaraldehyde in solution. In acidic conditions, glutaraldehyde exhibits stable performance [21,22].

On the other side, under our assay conditions (pH = 4), a cationized enzyme (pI 4.5) is possible by the presence of positively charged amines. In this way, the increasing number of primary amines provides for a greater number of molecules to be conjugated with glutaraldehyde. All these factors could be favored the cross linking between glutaraldehyde and different enzyme moieties [23].

These findings allow choosing pH of immobilization based not only upon their effectiveness environment for the best GA condition but also in their compatibility with the protein immobilized.

The coefficients R^2 and R^2 adjusted (R^2_{adj}) were 86.34% and 82.20%, respectively, meaning that 86.34% of the response variation is related to the variation of the independent variables. These coefficients emphasized that the model was highly significant and suitable for sufficient representation of the real relationship between these variables.

As a result, the optimal conditions for the lipase immobilization onto magnetic nanoparticles consisted of pH 3.7, enzyme concentration of 1.1 mg/mL at 4 °C and an ionic strength of 100 mM. The CRL@$MgFe_2O_4$ activity obtained was 3.2 times over the starting conditions (4.03 U/mL). There was a strong correlation obtained between the experimental 12.91 U/mL and predicted activity, 12.89 U/mL. Accordingly, the activity of the immobilized biocatalyst was optimized and improved.

The immobilization of the lipase on other similar supports was evaluated and compared to the activity of the free enzyme (Fig. 2B). Magnetite (Fe_3O_4), a support widely used for enzymes immobilization, was evaluated. Fig. 2B showed the activity of the CRL immobilized on Fe_3O_4 and $MgFe_2O_4$. The activity of the CRL@$MgFe_2O_4$ was 22% higher than free enzyme. This could be due to the high surface area provided by this support. The small size and non-porosity of these nanoparticles could allow lipase molecule to expand over the support surface with a better exposure of the active-site. These properties could may favor high binding capacity and improve the catalytic of the conjugated enzyme.

On the other hand, the activity of the CRL@$MgFe_2O_4$ was 61% higher than CRL@Fe_3O_4 (Fig. 2B). The difference between the lipase activities in both supports may be related to that the magnetite could have formed more agglomerates than the $MgFe_2O_4$, reducing thus its surface area. It is known that the smaller the nanoparticle, the higher is the ferromagnetism, and higher is the agglomeration [24]. Besides, the particle distance is much shorter, which increases magnetic dipole interparticle interactions that contribute to a heating process [24,25] and this could affect the lipase activity. Similar results using ferrites nanoparticles were observed by Klekotka et al. [10]. Thus, the size of the nanoparticles is a critical parameter that affects the lipase activity [4].

3.3. Characterization of CRL@$MgFe_2O_4$

3.3.1. FTIR

The covalent bond of lipase onto the magnetic support was corroborated by FTIR techniques. The FTIR spectra, for CRL, $MgFe_2O_4$ functionalized and CRL@$MgFe_2O_4$ are depicted in Fig. 3A.

The broad bands around 3400 and 1600 cm^{-1} in functionalized nanoparticles can be assigned to $-NH_2$ group (Fig. 3A). The peaks at 1500–1000 cm^{-1} refer to the symmetric stretching of Si—OH and Si—O—Si, respectively, which can be seen only for functionalized nanoparticles. This indicated that APTES has been coated on the surface of $MgFe_2O_4$.

The exact band position was determined by the backbone conformation and the hydrogen bonding pattern within the protein molecule, corresponding to 1600 cm^{-1} in the case of immobilized lipase and in the free enzyme a smooth difference was observed with a peak at

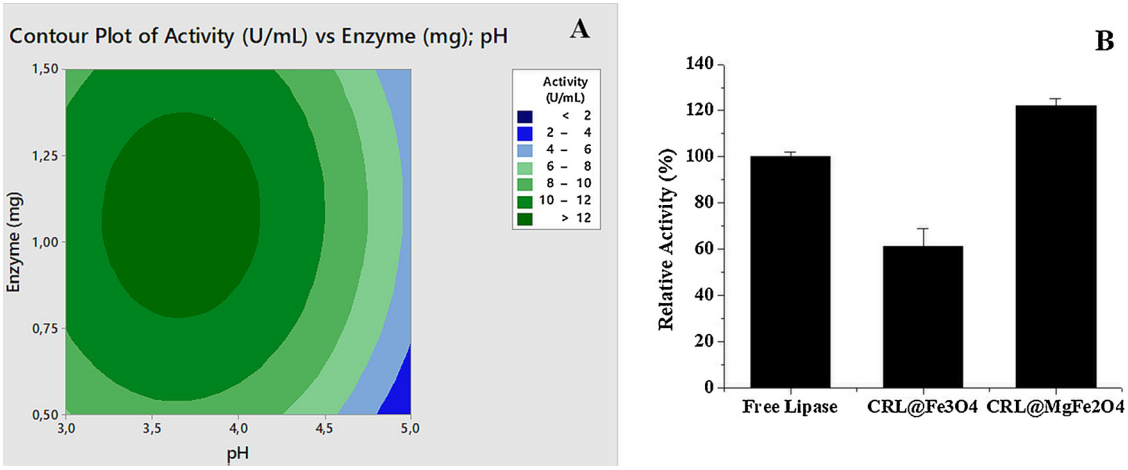

Fig. 2. A- Response surface and contour plots of the combined effects on Lipase activity of Enzyme concentration and pH. B- Comparison of the immobilization efficiency of the lipase using Fe_3O_4 or $MgFe_2O_4$ nanoparticles as supports.

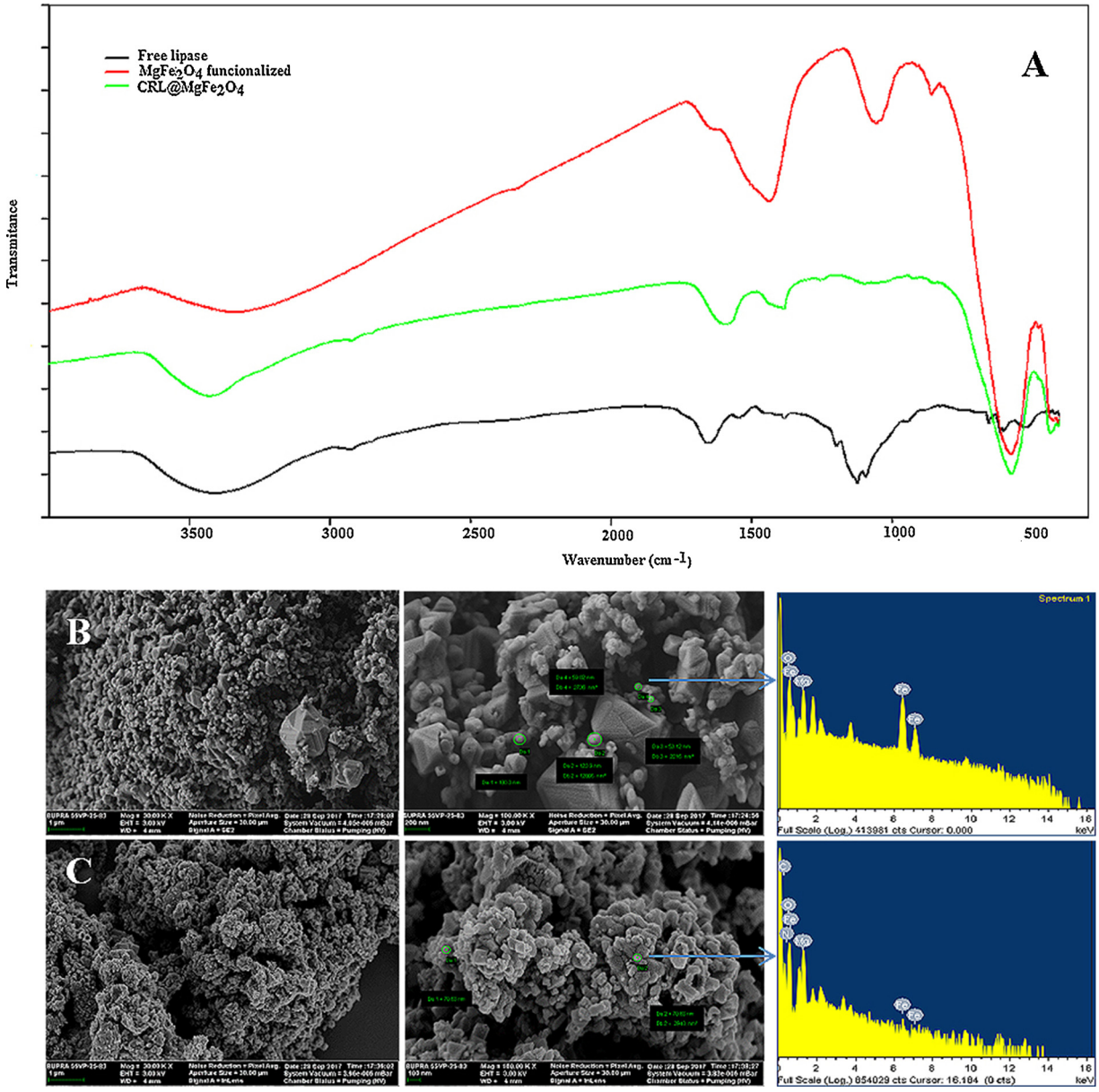

Fig. 3. A- FTIR spectra for CRL, $MgFe_2O_4$-funcionalized, and CRL@$FeMg_2O_4$. B- SEM (50.00 and 100.00 K ×) and EDS for Free $MgFe_2O_4$. C- SEM (50.00 and 150.00 K ×) and EDS for CRL@$FeMg_2O_4$.

1650 cm^{-1} (Fig. 3A). This difference could be due to conformational sensitivity of the Amide I band as consequence of the cross-linking [26]. The Amide II band occurs at 1500–1600 cm^{-1} and is mainly derived from the C—N stretch along with N—H in-plane bending. The appearance of peak at 1550 cm^{-1} only in the free lipase could be corresponding to this band [27].

Lastly, in free lipase, the Amide III band is found at 1200–1300 cm^{-1}. The vibrations responsible for this band are a complex mix of N—H bending and C—N stretching along with deformation vibrations of C—H and N—H [24]. At difference, in the immobilized lipase a very smooth peak was observed showing a conformational change in the protein. These results proved that lipase was immobilized successfully.

The bands assigned to Fe-O stretching and bending vibrations are observed at 577 and 433 cm^{-1}, in $MgFe_2O_4$ functionalized and CRL@$MgFe_2O_4$, this indicated the presence of the $MgFe_2O_4$ (Fig. 3A).

Thus, these results indicated that the CRL had been successfully tethered to the surface of $MgFe_2O_4$.

3.3.2. SEM-EDS

Free carrier nanoparticles (Fig. 3B) and CRL@$MgFe_2O_4$ (Fig. 3C) were subjected to SEM–EDS elemental analysis in order to verify the enzyme in the sample. In the SEM is possible observed the agglomerate that surrounds the iron-oxide core after the enzyme immobilization (Fig. 3C). Size of CRL@$MgFe_2O_4$ was estimated to be 70 nm in diameter. The EDS elemental analysis confirmed the presence of the enzyme in the CRL@$MgFe_2O_4$ through the presence of a peak of carbon atom (32% weight) and other for nitrogen (20%) (Table 1). These peaks were absent in the iron-oxides nanoparticles without enzyme as displayed by EDS (Fig. 3B). The atoms Fe and Mg were present in both the free nanoparticles and in CRL@$MgFe_2O_4$ as was detected by EDS (Fig. 3B and C). The O atom, present also in both, showed more % weight in the immobilized biocatalyst, 54.33% against 32.56% in the free nanoparticles (Table 1). In the first, the O atom could be contributed by oxide nanoparticle and for the enzyme also.

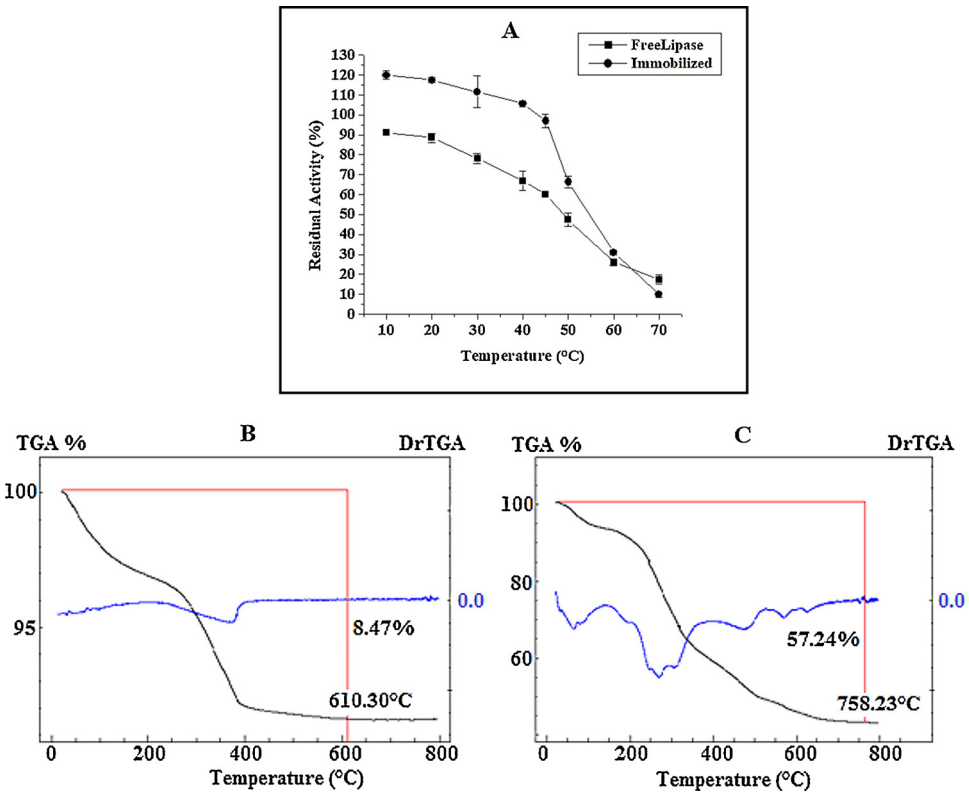

Fig. 4. A- Thermal stability of CRL@$FeMg_2O_4$ and free CRL. B- Thermogravimetric (TGA) analysis for CRL@$FeMg_2O_4$. C- TGA for free CRL.

3.4. Enzymatic properties

3.4.1. Thermal stability

The thermal stability assessment of the CRL@$MgFe_2O_4$ sowed a significant improvement at all the temperatures assayed compared with the free enzyme. A substantial enhancement was observed after the treatments between 10 and 50 °C, when the immobilized biocatalyst retained activity values of 20% and 45% superior to that of the free enzyme (Fig. 4A). These results suggest that the immobilized biocatalyst could outfit the immobilized enzymes against thermal denaturation.

The thermal properties of free lipase and CRL@$MgFe_2O_4$ were studied by thermogravimetric analysis (TGA) (Fig. 4B and C). Thermal analysis of the enzyme was measured as the function of temperature under controlled conditions. Analysis of thermograms in the case of enzyme immobilization studies is used to assess thermal stability [28] and to estimate the new structure of immobilized enzyme as well as efficacy of the enzyme immobilization method [29].

In Fig. 4 we show the Thermogravimetric Analysis (TGA, black line) and Thermogravimetric Derivative (DrTGA, blue line) of CRL@ $MgFe_2O_4$ (B) and free lipase (C). As can see the total weight loss in the (B) is 8.47%, much smaller than the loss in (C) that is 57.24%. This suggests that the lipase is stabilized after its immobilization.

In addition, in (B) the weight loss ends at 610.30 °C and in (C) at 758.23 °C suggesting that the immobilized enzyme is stabilized at a lower temperaturethus at a higher temperature the weight remains constant.

On the other hand, the derivative of the curve (B) has a single peak that indicates the process occurs in a step, in contrast, the derivate of (C) shows that the decomposition of free lipase occurs in several consecutive steps. This could be the reason of the major thermal stability of the lipase in immobilized condition. The CRL@$MgFe_2O_4$ was much more stable probably due to the increased rigidity and stability of the secondary structure after immobilization [30,28].

The immobilization may induce conformational changes in three-dimensional structure of the enzyme leading to a higher stability as compared to the free lipase [31,32].

Thus, the immobilization resulted in significantly higher thermal stability giving to CRL@$FeMg_2O_4$ an important potential advantage for practical applications in the industry [29,33].

3.4.2. pH stability

The effect of pH on the activity of the CRL@$MgFe_2O_4$ was determined in the range of pH 2–10 at 37 °C. As shown in Fig. 5A, the free lipase showed a similar residual activity (60–70%) in pH range tested between 2 and 8 with a loss of activity at more alkaline pH (9 and 10). When the lipase was immobilized in $MgFe_2O_4$ the behavior was similar in the same pH range, but the residual activity showed an increase of 20% more of activity than free enzyme. This effect was more noteworthy at alkaline pH, observing a 35% more of residual activity than free enzyme at pH 8 (Fig. 5A). Changes in the behavior at alkaline pH after the immobilization were observed also in the immobilized lipase B from *Candida antarctica* [34].

This change might be associated with the conformational change of enzyme on the carriers. On the other hand, the immobilization of the enzyme on the carriercould stabilize the pH of the microenvironment surrounding the enzyme, which plays an important role on the state of protonation of the protein molecule [32].

3.4.3. Solvent stability

Lipases are diverse in their sensitivity to solvents, but there is a general agreement that hydrophilic solvents are more destabilizing than hydrophobic solvents [35]. In this work, the immobilized enzyme showed a remarkable improved stability in the presence of hydrophilic solvents such as methanol or ethanol, since they retained between 15 and 45% of residual activity, more than the free enzyme, after of the exposure for 1 h at 37 °C in presence of hydrophilic solvents (Fig. 5B). The residual activity was falling as the length of the mono-alcohols chain increased, observing a strong loss of activity in the free enzyme in presence of butanol. However, the CRL@$MgFe_2O_4$ showed a residual

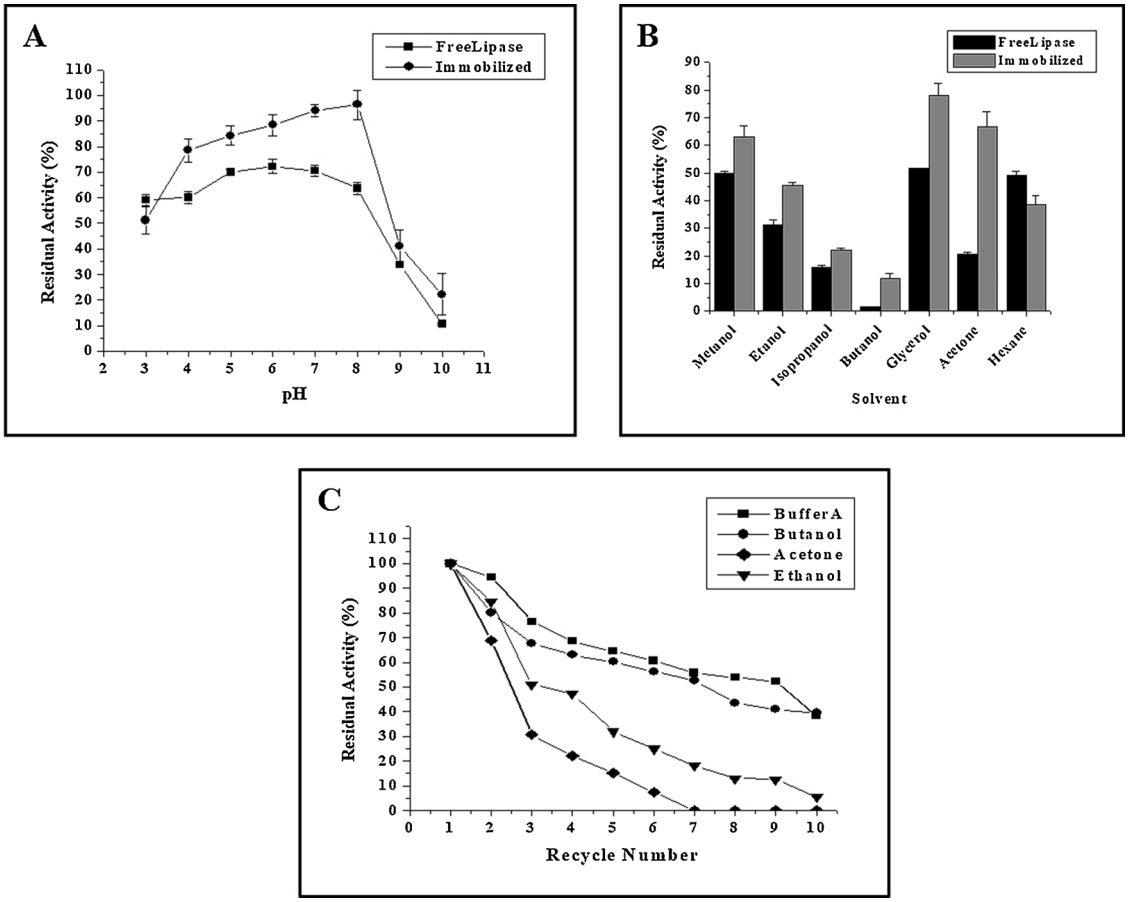

Fig. 5. Stability of CRL@$FeMg_2O_4$ and free CRL at pH (A) and Organic solvent (B). Reuse of CRL@$FeMg_2O_4$ after different wash treatments (C).

activity of 12% with the same alcohol (Fig. 5B). The best stability of the immobilized enzyme in front of hydrophilic solvents could be related to the presence of localized nanoenvironment granted by the support. The nanoenvironment surrounding enzyme molecules may prevent enzyme deactivation. A suitable environment may reduce the concentration of organic solvents near to the enzyme and prevent loss of enzyme activity [36].

The best organic solvent stability as consequence of the immobilization was observed in presence of glycerol (polyalcohol) and acetone with 26% and 46% more of residual activity than free enzyme (Fig. 5B). Polyols have proved to be enzymatic stabilizers via different mechanisms but considering that the high concentration that glycerol was used could have decreased of the water activity, a decrease of the mobility of the enzyme could have been the effect more relevant on its stability [37]. Thus, this reagent may be a good stabilizer of this enzyme under different conditions. Finally, in presence of n-hexane the free enzyme showed more stability than the CRL@$MgFe_2O_4$ (Fig. 5B).

3.4.4. Recycle of the biocatalyst

The CRL@$MgFe_2O_4$ was readily recycled by magnetic forces. The reusability of immobilized lipase after washing with different solvent is shown in Fig. 5C. The best recycling was obtained when any hydrophobic condition was used for the washing. Thus, the best residual activity was obtained when butanol or buffer with Triton X 100 (buffer A) were used (Fig. 5C).

After five repeated uses, CRL@$MgFe_2O_4$ recycled by washing with buffer A or butanol retained between 65 and 60% respectively and near 40% in the cycle ten for both solvent. Butanol was reported being effective in the regeneration of immobilized lipase possibly due to its ability to improve the negative effects of free fatty acid on activity [38,39]. This could also be the reason for the effect of buffer A, which, contain Triton X 100. The activity drop after five recycling can be partially attributed to the loss of lipase-bound nanoparticles. During recycling, the solution environment can disturb the enzyme conformation, and the nanoparticles slowly can lose the lipases molecules resulting in a decrease in the enzymatic activity [19]. As mentioned above the best environment for the enzyme was achieved in hydrophobic condition, in which probably, the enzyme conformation was conserved during more catalysis cycles.

In this case neither acetone nor ethanol showed to be good solvents for recycles of the biocatalyst, evidencing the positive effect of the hydrophobic nature of the solvents that were suitable for the washing and recycling of the biocatalyst.

3.5. Application of the biocatalyst

It is generally accepted that lipase-catalyzed hydrolytic activity does not usually correlate with its transesterification activity [2]. Thus, the performance of the CRL@$MgFe_2O_4$in hydrolysis and transesterification reaction was explored. In our initial experiments, we found that the immobilized enzyme hydrolyzed the triolein, observing mono and diglycerides. On the other hand, TLC presents several spots with different run front (Rf) which could be to fatty acid (Supplemental Material FS1 A).

The transesterification activities was evaluated also in reaction mixtures containing soy bean oil and ethanol in n-hexane shows new spots that could correspond to the ester production (FS1 B). Thus, we demonstrated the potential of CRL@$FeMg_2O_4$ as a potential biocatalyst for use in hydrolysis or synthesis reaction used both in several industrial processes.

3.6. Conclusion

In this work, magnesium ferrite nanoparticles were used as support for lipases immobilization. The lipase immobilization on magnesium ferrite showed more activity than in its free form and more than when was immobilized on magnetite. Thus, the physic-chemistry properties of the magnesium ferrite nanoparticles had a relevant effect on the lipase activity. The immobilized biocatalyst designed with the magnesium ferrite as support is a new generation biocatalyst with lipase activity. The immobilized lipase improved it stability at pH, hydrophilic solvent and temperature. From the thermogravimetric analysis was possible to observe that immobilization could induce conformational changes in three-dimensional structure of the enzyme leading to higher stability as compared to the free lipase. Consequently, the immobilization resulted in significantly higher thermal stability. The immobilized lipase was recycled by magnetic force application and used for more than five catalysis cycle, showing hydrolysis and synthesis activity. Thus, CRL@$FeMg_2O_4$ presents a potential advantage for industrial applications.

Acknowledgements

This work was supported by the following Argentine research grants 26D-517 PIUNT (UNT) and PIP 0677/2015CONICET.

Appendix A. Supplementary data

Supplementary material related to this article can be found, in the online version, at doi:https://doi.org/10.1016/j.colsurfb.2018.08.071.

References

[1] N. Sarmah, D. Revathi, G. Sheelu, K. Yamuna Rani, S. Sridhar, V. Mehtab, C. Sumana, Biotechnol. Prog. (2017), https://doi.org/10.1002/btpr.2581.
[2] C.M. Romero, L.M. Pera, F. Loto, C. Vallejos, G. Castro, M.D. Baigori, Biocatal. Agric. Biotechnol. 1 (2012) 25–31, https://doi.org/10.1016/j.bcab.2011.08.013.
[3] S. Cantone, V. Ferrario, L. Corici, C. Ebert, D. Fattor, P. Spizzo, L. Gardossi, Chem. Soc. Rev. 42 (2013) 6262, https://doi.org/10.1039/c3cs35464d.
[4] W. Shuai, R.K. Das, M. Naghdi, S.K. Brar, M. Verma, Biotechnol. Appl. Biochem. 64 (2017) 496–508, https://doi.org/10.1002/bab.1515.
[5] M. Chen, G. Zeng, P. Xu, C. Lai, L. Tang, Trends Biochem. Sci. 42 (2017) 914–930, https://doi.org/10.1016/j.tibs.2017.08.008.
[6] P. Zucca, E. Sanjust, Molecules 19 (2014) 14139–14194, https://doi.org/10.3390/molecules190914139.
[7] H. Vaghari, H. Jafarizadeh-Malmiri, M. Mohammadlou, A. Berenjian, N. Anarjan, N. Jafari, S. Nasiri, Biotechnol. Lett. 38 (2016) 223–233, https://doi.org/10.1007/s10529-015-1997-z.
[8] R. Dinali, A. Ebrahiminezhad, M. Manley-Harris, Y. Ghasemi, A. Berenjian, Crit. Rev. Microbiol. 43 (2017) 493–507, https://doi.org/10.1080/1040841X.2016.1267708.
[9] D. Yang, X. Wang, J. Shi, X. Wang, S. Zhang, P. Han, Z. Jiang, Biochem. Eng. J. 105 (2016) 273–280, https://doi.org/10.1016/j.bej.2015.10.003.
[10] U. Klekotka, M. Rogowska, D. Satuła, B. Kalska-Szostko, Beilstein J. Nanotechnol. 8 (2017) 1257–1265, https://doi.org/10.3762/bjnano.8.127.
[11] P. Holec, J. Plocek, D. Nižňanský, J. Poltierová Vejpravová, J. Sol.-Gel Sci. Technol. 51 (2009) 301–305, https://doi.org/10.1007/s10971-009-1962-x.
[12] K.W. Jung, S. Lee, Y.J. Lee, Bioresour. Technol. 245 (2017) 751–759, https://doi.org/10.1016/j.biortech.2017.09.035.
[13] U.K. Winkler, M. Stuckmann, J. Bacteriol. 138 (1979) 663–670, https://doi.org/10.1590/S0100-4042200800300030.
[14] M.M. Bradford, Anal. Biochem. 72 (1976) 248–254, https://doi.org/10.1016/0003-2697(76)90527-3.
[15] Y. Ichiyanagi, M. Kubota, S. Moritake, Y. Kanazawa, T. Yamada, T. Uehashi, J. Magn. Magn. Mater. 310 (2007) 2378–2380, https://doi.org/10.1016/j.jmmm.2006.10.737.
[16] Z. Wang, P. Lazor, S.K. Saxena, H.S.C. O'Neill, Mater. Res. Bull. 37 (2002) 1589–1602, https://doi.org/10.1016/S0025-5408(02)00819-X.
[17] Z.J. Zhang, Z.L. Wang, B.C. Chakoumakos, J.S. Yin, J. Am. Chem. Soc. 120 (1998) 1800–1804, https://doi.org/10.1021/ja973085l.
[18] M.I. Gómez, G. Lucotti, J.A. Morán, P. Aymonio, S. Pagola, P. Stephens, R. Carbonio, J. Solid State Chem. 160 (2001) 17–24, https://doi.org/10.1006/jssc.2001.9119.
[19] J. Feng, S. Yu, J. Li, T. Mo, P. Li, Chem. Eng. J. 286 (2016) 216–222, https://doi.org/10.1016/j.cej.2015.10.083.
[20] H. Kim, J. Kwon, RSC Adv. 7 (2017) 19656–19661, https://doi.org/10.1039/c7ra01615h.
[21] A.F.S.A. Habeeb, R. Hiramoto, Arch. Biochem. Biophys. 126 (1968) 16–26.
[22] I. Migneault, C. Dartiguenave, M.J. Bertrand, K.C. Waldron, BioTechniques 37 (2004) 790–802, https://doi.org/10.2144/3705A0790.
[23] E.-K. Yan, H.-L. Cao, C.-Y. Zhang, Q.-Q. Lu, Y.-J. Ye, J. He, L.-J. Huang, D.-C. Yin, RSC Adv. 5 (2015) 26163–26174, https://doi.org/10.1039/C5RA01722J.
[24] B. Issa, I.M. Obaidat, B.A. Albiss, Y. Haik, Int. J. Mol. Sci. 14 (2013) 21266–21305, https://doi.org/10.3390/ijms141121266.
[25] U. Engelmann, E.M. Buhl, M. Baumann, T. Schmitz-rode, Curr. Directions Biomed. Eng. 3 (2017) 457–460, https://doi.org/10.1515/cdbme-2017-0096.
[26] S.E. Glassford, B. Byrne, S.G. Kazarian, Biochim. Biophys. Acta - Proteins Proteom. 1834 (2013) 2849–2858, https://doi.org/10.1016/j.bbapap.2013.07.015.
[27] W. Xie, X. Zang, Food Chem. 227 (2017) 397–403, https://doi.org/10.1016/j.foodchem.2017.01.082.
[28] A. Dwevedi, Enzym. Immobil. Adv. Ind. Agric. Med. Environ. (2016) 1–132, https://doi.org/10.1007/978-3-319-41418-8.
[29] N.R. Mohamad, N.H.C. Marzuki, N.A. Buang, F. Huyop, R.A. Wahab, Biotechnol. Biotechnol. Equip. 29 (2015) 205–220, https://doi.org/10.1080/13102818.2015.1008192.
[30] K.A. Mahmoud, E. Lam, S. Hrapovic, J.H.T. Luong, ACS Appl. Mater. Interfaces 5 (2013) 4978–4985, https://doi.org/10.1021/am4007534.
[31] S.A. Ansari, Q. Husain, Biotechnol. Adv. 30 (2012) 512–523, https://doi.org/10.1016/j.biotechadv.2011.09.005.
[32] B.J. Johnson, W. Russ Algar, A.P. Malanoski, M.G. Ancona, I.L. Medintz, Nano Today 9 (2014) 102–131, https://doi.org/10.1016/j.nantod.2014.02.005.
[33] S.L. Cao, Y.M. Huang, X.H. Li, P. Xu, H. Wu, N. Li, W.Y. Lou, M.H. Zong, Sci. Rep. 6 (2016) 1–12, https://doi.org/10.1038/srep20420.
[34] X. Wan, X. Xiang, S. Tang, D. Yu, H. Huang, Y. Hu, Colloids Surfaces B Biointerfaces 160 (2017) 416–422, https://doi.org/10.1016/j.colsurfb.2017.09.037.
[35] L.M. Pera, C.M. Romero, M.D. Baigori, G.R. Castro, Food Technol. Biotechnol. 44 (2006) 247–252.
[36] M. Misson, H. Zhang, B. Jin, J. R. Soc. Interface 12 (2014), https://doi.org/10.1098/rsif.2014.0891 40891 – 20140891.
[37] H. Zaak, L. Fernandez-Lopez, C. Otero, M. Sassi, R. Fernandez-Lafuente, Enzyme Microb. Technol. 106 (2017) 67–74, https://doi.org/10.1016/j.enzmictec.2017.07.001.
[38] C.Y. Yu, L.Y. Huang, I.C. Kuan, S.L. Lee, Int. J. Mol. 14 (2013) 24074–24086, https://doi.org/10.3390/ijms141224074.
[39] E.C.G. Aguieiras, D.S. Ribeiro, P.P. Couteiro, C.M.B. Bastos, D.S. de Queiroz, J.M. Parreira, M.A.P. Langone, Appl. Biochem. Biotechnol. 179 (2016) 485–496, https://doi.org/10.1007/s12010-016-2008-9.